Journal of Organometallic Chemistry, 358 (1988) 347–361
Elsevier Sequoia S.A., Lausanne – Printed in The Netherlands

Diiron μ-vinylcarbyne complexes have unusually low barriers to vinyl rotation because conjugation is maintained throughout rotation

Charles P. Casey *, Mark S. Konings, Seth R. Marder, and Yoshiaki Takezawa
Department of Chemistry, University of Wisconsin, Madison, WI 53706 (U.S.A.)

(Received April 18th, 1988)

Abstract

Rotational barriers of diiron μ-vinylcarbyne complexes were measured by temperature dependent ^1H and ^{13}C NMR line shape analysis. The planar vinylcarbyne ligand in $[C_5H_5(CO)Fe]_2(\mu\text{-CO})[\mu\text{-C-}E\text{-CH=CHC}_6H_4\text{-}p\text{-N(CH}_3)_2]^+BF_4^-$ (**5**) was found to possess three measurable rotational barriers. Rotation of the entire vinylcarbyne ligand has the lowest barrier to rotation, $\Delta G^{\ddagger}_{218}$ 10.6(1) kcal mol^{-1}. Rotation of the $N(CH_3)_2$ group has a barrier of $\Delta G^{\ddagger}_{210}$ 10.9(1) kcal mol^{-1}, and rotation of the aryl group has a barrier of $\Delta G^{\ddagger}_{275}$ 13.0(1) kcal mol^{-1}. Fenske–Hall molecular orbital calculations reveal that diiron vinylcarbyne complexes have low barriers to ligand rotation because the bridging carbyne carbon has orthogonal *p* orbitals which can accept electron density from the vinyl unit throughout rotation.

We recently developed two efficient synthetic routes into cationic μ-vinylcarbynediiron complexes. The first utilizes the condensation of cationic μ-alkylidynediiron complexes with aldehydes, ketones, and *ortho* esters [1]. The key step in these condensations is proposed to be attack of a carbon electrophile (such as protonated aldehyde) on the electron rich double bond of a neutral μ-alkenylidenediiron complex in equilibrium with a cationic μ-alkylidyne precursor. A second route into μ-vinylcarbyne complexes involves hydride abstraction from a μ-alkenylidene complex [2].

μ-Vinylcarbyne complexes are useful synthetic intermediates in the synthesis of functionalized μ-alkenylidene complexes. Nucleophiles such as $NaCH(CO_2CH_2CH_3)_2$ and PMe_3 add regioselectively to the remote vinyl carbon atom of μ-vinylcarbyne complexes to generate μ-alkenylidene complexes [3].

In the X-ray crystal structure of $[C_5H_5(CO)Fe]_2(\mu\text{-CO})(\mu\text{-C-}E\text{-CH=CHC}_6H_4\text{-}p\text{-CH}_3)^+BF_4^-$ (**2**) [1] the two iron centers, the vinylcarbyne ligand, and the aryl ring lie approximately in the same plane (Fig. 1). The vinylcarbyne ligand is best described as having a single bond (1.422(8) Å) between the μ-alkylidyne carbon and

0022-328X/88/$03.50

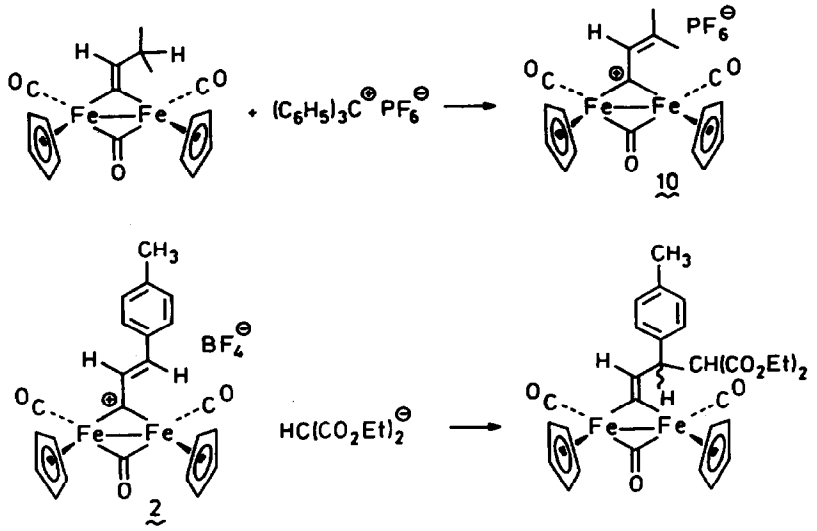

the vinyl group and a localized double bond (1.335(8) Å) in the vinyl unit. The planar geometry of the diiron vinylcarbyne unit allows effective conjugation of the double bond and the aryl group with an electron deficient μ-carbyne p-orbital perpendicular to the planar system.

The non-equivalent cyclopentadienyl (η-C_5H_5, Cp) groups of **2** give rise to only a single Cp resonance at δ 5.67 in the ^1H NMR and at δ 93.1 in ^{13}C NMR spectra at room temperature. This implies that a rapid fluxional process, such as rotation of the vinylcarbyne ligand, exchanges the environments of the two Cp ligands.

Here we report variable temperature NMR studies of vinylcarbyne complexes

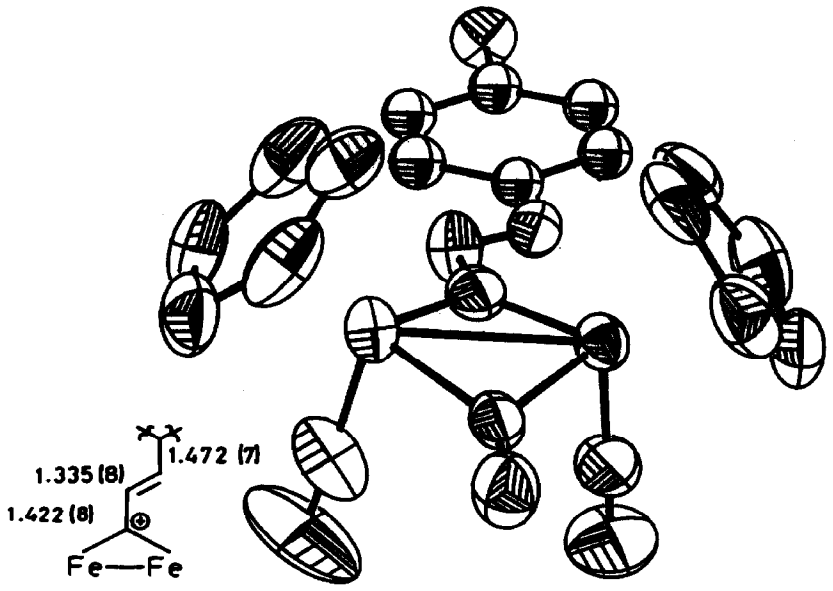

Fig. 1. Structure of 2. BF_4^- and hydrogens omitted for clarity.

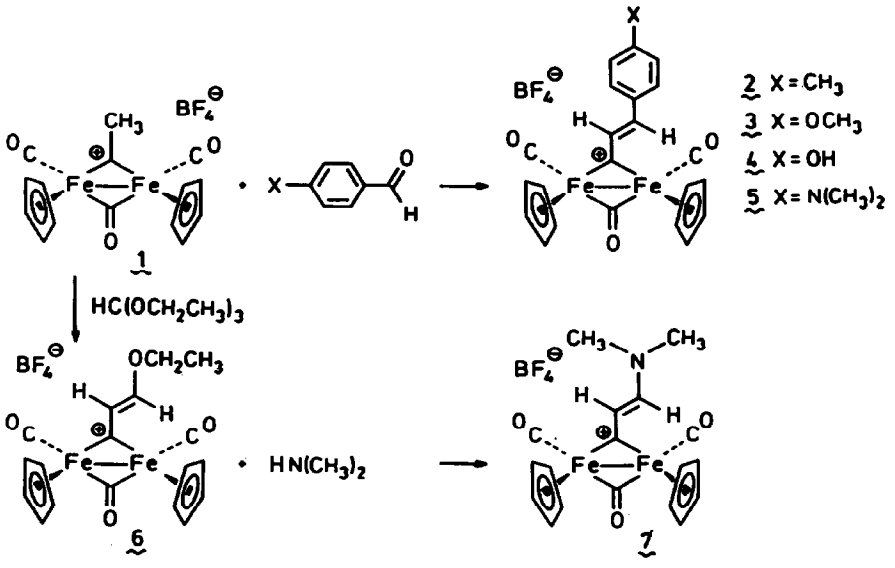

Scheme 1

that indicate unusually low barriers to rotation of the vinylcarbyne ligand. In the case of $[C_5H_5(CO)Fe]_2(\mu\text{-}CO)[\mu\text{-}C\text{-}E\text{-}CH{=}CHC_6H_4\text{-}p\text{-}N(CH_3)_2]^+BF_4^-$ (**5**), the barrier to rotation of the vinyl group ($\Delta G^{\ddagger}$ 10.6(1) kcal mol^{-1}) is even lower than the barrier to rotation of the aryl ring ($\Delta G^{\ddagger}$ 13.0(1) kcal mol^{-1}). The higher barrier for aryl rotation than for vinyl rotation is an experimental indication that the vinyl group remains in conjugation with the Fe_2–μ-C unit throughout rotation. Fenske–Hall molecular orbital calculations [4] provide a useful framework for understanding this phenomenon.

Synthesis of vinylcarbyne complexes. Aryl substituted vinylcarbyne complexes **2–5** were prepared in high yields (> 80%) by the condensation of ethylidynediiron complex $[C_5H_5(CO)Fe]_2(\mu\text{-}CO)(\mu\text{-}C\text{-}CH_3)^+BF_4^-$ (**1**) [5] with *para*-substituted benzaldehydes. Condensation of triethyl orthoformate with **1** led to the formation of the vinyl ether carbyne complex $[C_5H_5(CO)Fe]_2(\mu\text{-}CO)(\mu\text{-}C\text{-}E\text{-}CH{=}CHOEt)^+BF_4^-$ (**6**). Reaction of **6** with dimethylamine produced the amine substituted vinylcarbyne complex $[C_5H_5(CO)Fe]_2(\mu\text{-}CO)[\mu\text{-}C\text{-}E\text{-}CH{=}CHN(CH_3)_2]^+BF_4^-$ (**7**). These results are summarized in Scheme 1. Full details of the synthesis of these vinylcarbyne complexes will be presented elsewhere [6a].

Rotational barriers in vinylcarbyne complexes. The results of variable temperature NMR studies outlined below indicate that the barrier to rotation about the bond between the carbyne carbon and the vinyl unit increases as better electron donor groups are placed on the remote vinyl carbon. The vinylcarbyne complexes with the best donor substituents and the highest barriers will be discussed first.

The X-ray crystal structure of the dimethylamino substituted vinylcarbyne complex 7 [6b*] shows that the two iron centers, the vinylcarbyne unit, and the dimethylamino group lie approximately in the same plane (Fig. 2). The maximum deviation from the mean plane is the 0.11 Å displacement of C(7). The similar

* Reference number with asterisk indicates a note in the list of references.

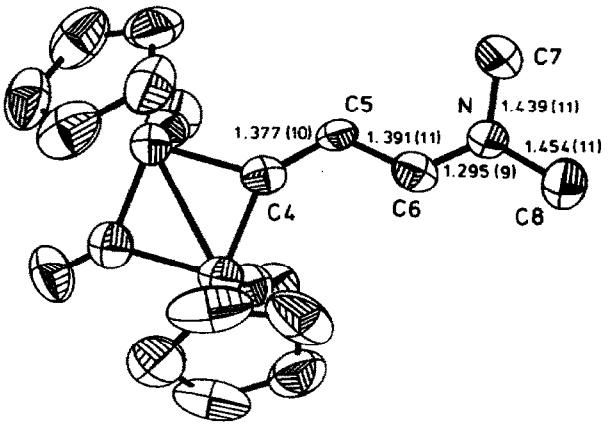

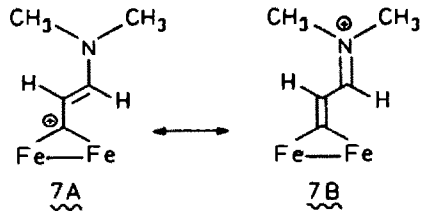

Fig. 2. Structure of **7**. BF_4^- and hydrogens omitted for clarity.

carbon–carbon bond lengths in the vinylcarbyne group (C(4)–C(5), 1.377(10) Å; C(5)–C(6), 1.391(11) Å) and the short bond from the amino nitrogen to the vinyl carbon (N–C(6), 1.295(9) Å) indicate the importance of resonance structures **7A** and **7B**.

The *cis*-Cp groups of **7** are clearly in different environments and give rise to separate resonances at δ 5.16 and 5.14 in the ^{1}H NMR spectrum in CD_3CN at room temperature. As the temperature is raised, the two resonances for the Cp groups broaden and coalesce into a single peak at δ 5.15 at 93°C. Complete line shape analysis in the temperature range 76 to 112°C established a vinyl rotational barrier of $\Delta G^{\ddagger}$ 19.8(1) kcal mol^{-1}, $\Delta H^{\ddagger}$ 20.5(6) kcal mol^{-1}, and $\Delta S^{\ddagger}$ 2(2) e.u. Separate *N*-methyl resonances were seen at δ 3.57 and 3.49 at 112°C which indicates a high barrier to rotation about the carbon–nitrogen bond. From the observed line widths, a rate of exchange of < 1 sec^{-1} was estimated which corresponds to $\Delta G^{\ddagger} > 22.7$ kcal mol^{-1} at 112°C.

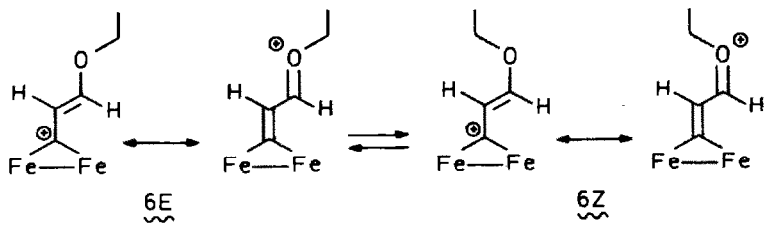

A 2.3/1.0 ratio of two isomers of the vinyl ether carbyne complex **6** was observed by ^{1}H NMR at −110°C. Two Cp resonances were observed for each isomer. In the 270 MHz spectrum, the Cp resonances of the major isomer appeared at δ 5.60 and

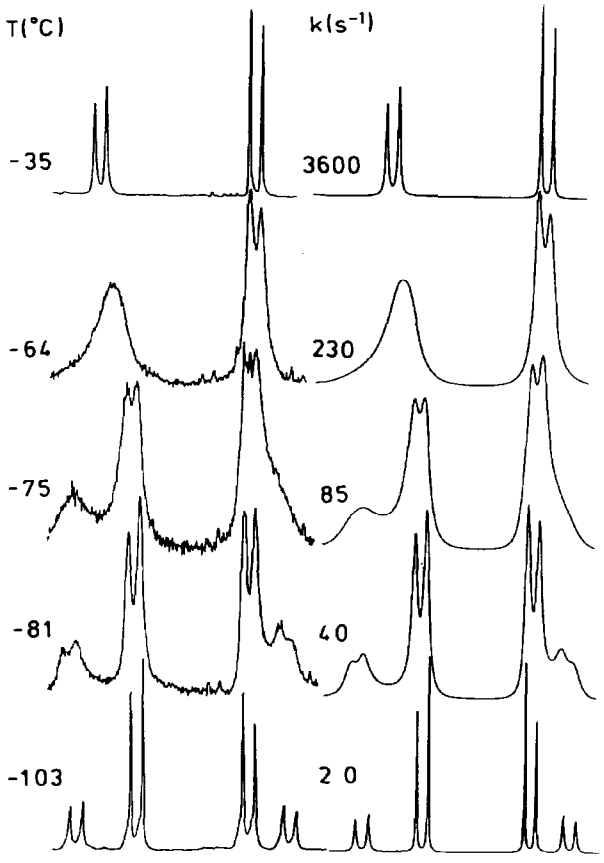

Fig. 3. 270 MHz variable temperature ^{1}H NMR spectra of the vinyl region of **6**. Observed spectra and temperatures are on the left. Simulated spectra and rates are on the right.

5.58 while those of the minor isomer appeared at δ 5.64 and 5.61. Two vinyl doublets were observed for each isomer at $-110\,^\circ$C. The major isomer has resonances at δ 9.19 (d, J 10.7 Hz, μ-C–CH) and 8.83 (d, J 10.7 Hz, μ-C–CH=C*H*) while the minor isomer has resonances at δ 9.40 (d, J 11.4 Hz, μ-C–CH) and 8.68 (d, J 11.4 Hz, μ-C–CH=C*H*). The infrared spectrum of **6** has terminal CO stretches at 2032(s) and 2000(m) cm^{-1} consistent with *cis* terminal CO ligands [7]. Restricted rotation about the C–O bond of the vinyl ether gives rise to isomers **6E** and **6Z** in which the ethyl group is either *trans* or *cis* to the carbon chain of the vinylcarbyne group. In each isomer, the entire vinyl ether carbyne unit is planar and the Cp ligands of each isomer are in different environments. Line shape analysis of the variable temperature spectra (Fig. 3) indicated a barrier of $\Delta G^\ddagger$ 9.7(2) kcal mol^{-1}, $\Delta H^\ddagger$ 8.2(1) kcal mol^{-1}, and $\Delta S^\ddagger$ -8(1) e.u. for this process. This coalescence behavior is attributed to rotation about the C–O bond of the vinyl ether that interconverts the major and minor isomers.

This same process is responsible for the coalescence of the Cp resonances of **6** (Fig. 4). As the temperature was increased, the low field resonances of the major and minor isomers at δ 5.64 and 5.60 coalesced into a peak at δ 5.57 while the high field resonances of the major and minor isomers at δ 5.61 and 5.58 coalesced into a peak at δ 5.54. At $-75\,^\circ$C, rotation about the carbyne–carbon to vinyl–carbon

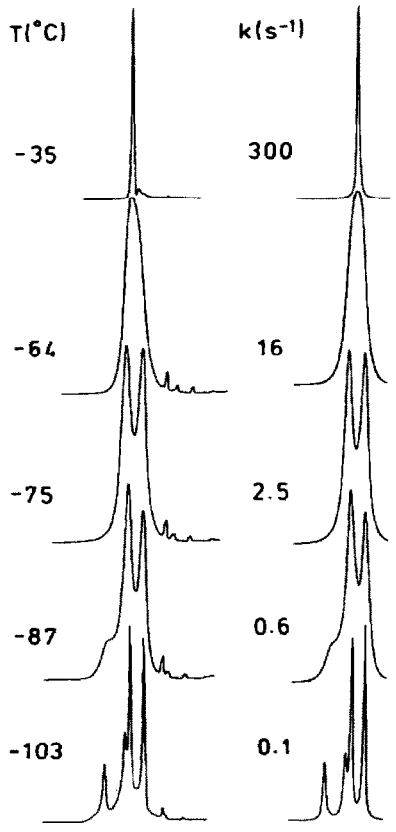

Fig. 4. 270 MHz variable temperature ^{1}H NMR spectra of the Cp region of **6**. Observed spectra and temperatures are on the left. Simulated spectra and rates are on the right.

bond is slow and the rapidly equilibrating mixture of **6Z** and **6E** still has two different Cp resonances. From line shape analysis of the spectra, $\Delta G^{\ddagger}$ 11.0(1) kcal mol^{-1}, $\Delta H^{\ddagger}$ 10.6(4) kcal mol^{-1}, and $\Delta S^{\ddagger}$ −2(2) e.u. were calculated for this second fluxional process which is attributed to rotation about the carbyne carbon to vinyl carbon bond. There are some uncertainties in our estimates of these rotational barriers due to the complexity of the system and to our inability to fully take into account the temperature dependence of the chemical shifts of the vinyl and Cp resonances. Nevertheless, the barrier to rotation about the carbyne carbon to vinyl carbon bond is substantially lower than that of the nitrogen substituted vinylcarbyne complex **7**. This is readily understood in terms of the greater electron donating ability of the dimethylamino group compared with the ethoxy group.

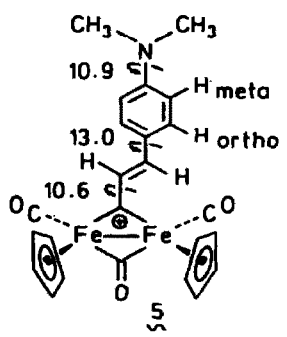

5

The low temperature ^{1}H NMR spectrum of the *p*-dimethylaminophenyl substituted vinylcarbyne complex **5** established the flat geometry of this ligand system and indicated the presence of three different rotational barriers which are readily understood in terms of a planar conjugated system extending from the carbyne carbon out to the dimethylamino group. We measured these three barriers by observing three independent dynamic NMR processes. Rotation of the entire vinylcarbyne group interchanges the environments of the Cp groups on iron and remarkably was found to have the lowest barrier to rotation. A barrier to vinyl rotation of $\Delta G^{\ddagger}$ 10.7(2) kcal mol^{-1} at $-73\,^{\circ}$C was calculated from the coalescence behavior. Separate, sharp Cp resonances were also observed for **5** in the 126 MHz ^{13}C NMR spectrum at δ 91.44 and 91.05 at $-76\,^{\circ}$C. Line shape analysis in the temperature range of -71 to $-34\,^{\circ}$C indicated a barrier to rotation of $\Delta G^{\ddagger}$ 10.6(1) kcal mol^{-1} ($\Delta H^{\ddagger}$ 10.0(2) kcal mol^{-1}, $\Delta S^{\ddagger}$ -3(1) e.u.) which is within experimental error of the value obtained from the coalescence temperature in the ^{1}H NMR spectrum.

A rotational barrier for the NMe_2 group of $\Delta G^{\ddagger}$ 10.9(1) kcal mol^{-1} at $-63\,^{\circ}$C was calculated from the coalescence behavior of the *N*-methyl resonances.

Separate resonances for the *meta* and *meta'* hydrogens and for the *ortho* and *ortho'* hydrogens made it possible to use two independent measures of the aryl rotation barrier. A barrier to rotation of the aryl group of $\Delta G^{\ddagger}$ 13.0(1) kcal mol^{-1} at $-15\,^{\circ}$C was estimated from the coalescence behavior of the *meta* hydrogens; a barrier of $\Delta G^{\ddagger}$ 13.0(1) kcal mol^{-1} at $2\,^{\circ}$C was estimated from the coalescence behavior of the *ortho* hydrogens.

The temperature dependent NMR spectra of aryl substituted vinylcarbyne complexes $[C_5H_5(CO)Fe]_2(\mu\text{-CO})(\mu\text{-C-}E\text{-CH=CHC}_6H_4\text{-}p\text{-OH})^+BF_4^-$ (**4**), $[C_5H_5(CO)Fe]_2(\mu\text{-CO})(\mu\text{-C-}E\text{-CH=CHC}_6H_4\text{-}p\text{-OCH}_3)^+BF_4^-$ (**3**), and $[C_5H_5(CO)Fe]_2(\mu\text{-CO})(\mu\text{-C-}E\text{-CH=CHC}_6H_4\text{-}p\text{-CH}_3)^+BF_4^-$ (**2**) were also studied. In these cases, only a single Cp resonance was seen in the ^{1}H NMR for each of these compounds even at low temperature and high magnetic field ($-106\,^{\circ}$C, 270 MHz for **4**; $-104\,^{\circ}$C, 270 MHz for **3**; $-100\,^{\circ}$C, 500 MHz for **2**). In the 50 MHz ^{13}C NMR spectrum of **4** at $-80\,^{\circ}$C, only a single Cp resonance and a single terminal CO resonance were observed. These results are consistent with a low barrier for vinyl rotation.

The low temperature ^{1}H NMR spectra of **2**, **3**, and **4** revealed a barrier to aryl rotation that depended on the electron donor ability of the *para* substituent. For the *p*-hydroxyphenyl complex **4**, coalescence of the *ortho* and *ortho'* protons and of the *meta* and *meta'* protons allowed two independent measurements of the aryl rotation barrier. For the *p*-tolyl complex **2**, and the *p*-methoxyphenyl complex **3**, only protons *ortho* to the vinyl group had separate resonances in the low temperature limiting spectra. The protons *meta* to the vinyl group appeared as broadened resonances, presumably because the chemical shifts between the *meta* and *meta'* protons is not great enough to allow differentiation in the low temperature limiting spectra.

For the *p*-tolyl complex **2**, coalescence of the aromatic protons was also analyzed by line shape analysis in the temperature range -100 to $-48\,^{\circ}$C. $\Delta G^{\ddagger}$ 8.3(1) kcal mol^{-1} ($\Delta H^{\ddagger}$ 9.0(2) kcal mol^{-1}, $\Delta S^{\ddagger}$ 4(1) e.u.) was calculated from these data. This barrier is very similar to that calculated from the coalescence temperature ($\Delta G^{\ddagger}$ 8.4(1) kcal mol^{-1}, $-88\,^{\circ}$C), and indicates that in this case no significant error was introduced in calculating $\Delta G^{\ddagger}$ from the coalescence temperature by using equations for singlets [8].

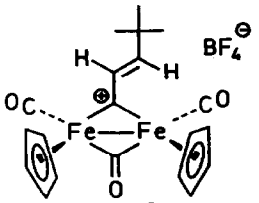

8

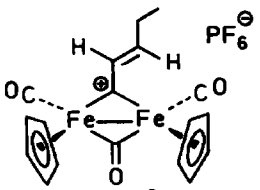

9

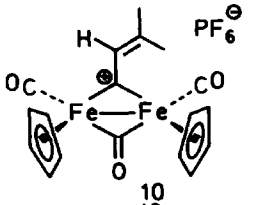

10

The low temperature ^{1}H NMR spectra of the alkyl substituted vinylcarbyne complexes **8** [1], **9** [2], **10** [1,2] showed only one Cp resonance. Apparently, these compounds also have very low barriers to vinyl rotation.

Discussion

Variable temperature NMR studies on diiron vinylcarbyne complexes reveal a low barrier to rotation of the carbyne carbon to vinyl carbon bond (Table 1). Entropies of activation were generally found to be near zero, consistent with a simple rotational process. The vinyl rotational barrier is only observable when a good electron donor substituent is attached to the remote vinyl carbon as in the NMe_2 (**7**), OEt (**6**), and C_6H_4-*p*-NMe_2 (**5**) substituted complexes. No barrier to vinyl rotation was observed for compounds with less powerful donor substituents such as C_6H_4-*p*-CH_3 (**2**), C_6H_4-*p*-OMe (**3**), C_6H_4-*p*-OH (**4**), CMe_3 (**8**), Et (**9**), Me_2 (**10**). Table 1 indicates that the magnitude of the vinyl rotational barrier is greatest for the compounds with the strongest electron donor substituents. These vinylcarbyne rotational barriers are substantially lower than barriers to rotation in organic allyl cations (Table 2) [9].

Aryl substituted vinylcarbyne complexes **2–5** were found to possess a substantial barrier to rotation of the aryl group. Table 3 indicates that the magnitude of the aryl rotation barrier is increased by electron donating *para* substituents. For the *p*-dimethylaminophenyl substituted vinylcarbyne complex **5**, the rotational barrier of the aryl ring, $\Delta G^{\ddagger}$ 13.0(1) kcal mol^{-1}, is much greater than the barrier to rotation of the entire vinylcarbyne unit, $\Delta G^{\ddagger}$ 10.6(1) kcal mol^{-1}. Aryl rotational barriers of vinylcarbyne complexes are similar to the rotational barriers observed for *para* substituted benzaldehydes [10].

Table 1

μ-Vinylcarbyne rotational barriers

R	$\Delta G^{\ddagger}$ [a]
$N(CH_3)_2$	19.8(1) [b]
OCH_2CH_3	11.0(1) [b]
C_6H_4-*p*-$N(CH_3)_2$	10.6(1) [c], 10.7(2) [d]
C_6H_4-*p*-OH	< 8.4 [e]
C_6H_4-*p*-OCH_3	< 8.4 [e]
C_6H_4-*p*-CH_3	< 8.0 [e]

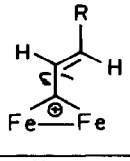

[a] In kcal mol^{-1}. [b] From ^{1}H NMR line shape analysis. [c] From ^{13}C NMR line shape analysis. [d] From ^{1}H NMR coalescence temperature. [e] Assumes Cp and Cp′ chemical shift difference the same as observed for **5**.

Table 2

Allyl cation rotation barriers [a]

Allyl cation	$\Delta G^{\ddagger}$ [b]
$CH_2{=}CH{=}CH_2$	23.7 [c]
Z,E-MeCH=CH=CHMe	22.4
Z,Z-MeCH=CH=CHMe	18.7
Z,E-MeCH=CMe=CHMe	23.6
Z,Z-MeCH=CMe=CHMe	18.1
E-$Me_2C{=}CMe{=}CHMe$	15.8
$Me_2C{=}CMe{=}CMe_2$	13.8

[a] Values are from ref. 9a. [b] In kcal mol^{-1}. [c] Calculated value taken from ref. 9b.

The higher barrier to rotation of the aryl group than of the entire vinylcarbyne ligand is direct experimental evidence that the planar vinylcarbyne ligand remains in conjugation with the electron deficient bridging carbyne carbon throughout rotation of the vinylcarbyne ligand.

The X-ray crystal structure of the *p*-tolyl substituted vinylcarbyne complex **2** and of the dimethylamino-substituted vinylcarbyne complex **7** establish the planar nature of the vinylcarbyne ligand. In this conformation, conjugation of the double bond and the aryl or amino group with an electron deficient μ-alkylidyne carbon *p*-orbital perpendicular to the planar system is maximized. In order to determine how conjugation between the vinylcarbyne ligand and the μ-alkylidyne carbon is maintained throughout ligand rotation, we examined the bonding in vinylcarbyne complexes using Fenske–Hall molecular orbital calculations [4].

Calculations were performed on the unsubstituted vinylcarbyne complex using atomic coordinates obtained from the X-ray crystal structure of the related aryl substituted vinylcarbyne complex **2** (Fig. 5). We call this geometry the planar conformation. Additional calculations were performed on the perpendicular conformations resulting from 90° rotation of the vinylcarbyne ligand both towards and away from the terminal carbonyls. Since no significant differences were found between calculations of the two different perpendicular conformations, we will discuss only the conformation with the vinyl group *cis* to the terminal CO ligands.

Table 3

Aryl rotation barriers

X	$\Delta G^{\ddagger}$ [a]
$N(CH_3)_2$	13.0(1) [b], 13.0(1) [c]
OH	9.8(1) [b], 9.8(1) [c]
OCH_3	9.4(1) [b]
CH_3	8.3(1) [d], 8.4(1) [b]

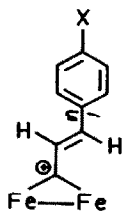

[a] In kcal mol^{-1}. [b] From ^1H NMR coalescence of the *ortho* and *ortho'* hydrogens. [c] From ^1H NMR coalescence of the *meta* and *meta'* hydrogens. [d] From ^1H NMR line shape analysis.

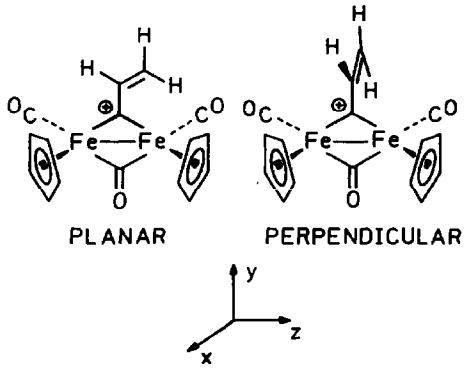

Fig. 5. Planar (left) and perpendicular (right) geometries used in Fenske–Hall calculations along with the coordinate system used. The coordinate system is chosen to be identical for all atoms in both conformations.

In the discussion to follow, the atomic coordinates on all atoms are chosen to be identical to one another and are as indicated by the coordinate system given in Fig. 5.

There are three important occupied vinylcarbyne ligand orbitals in the planar conformation which will be discussed in order of increasing energy. The first orbital has significant π-bonding contributions from p_x atomic orbitals on the bridging carbyne carbon and vinyl carbon atoms (Fig. 6a). This orbital is formed predominantly from p_x orbitals on the three vinylcarbyne carbons: C(4), 30%; C(5), 34%; and C(6), 18% and has small π-bonding contributions (9%) from iron d_{xy} and d_{xz} orbitals. This orbital is similar to the lowest energy orbital of the allyl cation. The second ligand orbital has σ-bonding contributions from the p_z orbital located on the bridging carbyne carbon (28%) and d_{yz}, $d_{x^2-y^2}$, and d_{z^2} iron orbitals (37%) (Fig. 6b). The third important orbital in the planar conformation has π-character from two iron d_{xz} orbitals (47%) and the C(4) p_x orbital (10%) (Fig. 6c). A node exists between C(4) and C(5), while the in-phase C(5) and C(6) p_x orbitals contribute to 18% of its character.

When the vinylcarbyne ligand is rotated by 90° to the perpendicular conformation, three occupied vinylcarbyne ligand orbitals are generated. The lowest energy orbital is a bonding combination of the carbyne p_z orbital (41%) and the π-bond of the vinyl group (32%) (Fig. 7a). The second orbital is π-antibonding between the carbyne p_z orbital (7%) and the vinyl π-bond (63%) and is π-bonding between the carbyne p_z orbital and the $d_{x^2-y^2}$ and d_{yz} iron orbitals (20%) (Fig. 7b). The third orbital involves π-bonding between the carbyne p_x orbital (18%) and iron d_{xz} orbitals (42%) (Fig. 7c).

The carbyne carbon atom has a p_x orbital perpendicular to the Fe_2–μ-C unit and a p_z orbital in the plane of the Fe_2–μ-C unit and parallel to the Fe–Fe vector. In the planar conformation, the p_x orbital is involved in π-bonding (Fig. 6a) and π-antibonding (Fig. 6c) combinations with the vinyl π-bond and the p_z orbital is involved in σ-bonding to iron (Fig. 6b). Upon rotation of the vinyl group by 90° to the perpendicular conformation, the roles of the carbyne p_x and p_z orbitals are reversed. The p_z orbital now forms a bonding (Fig. 7a) and an anti-bonding (Fig. 7b) combination with the vinyl group and the p_x orbital is involved in π-bonding to

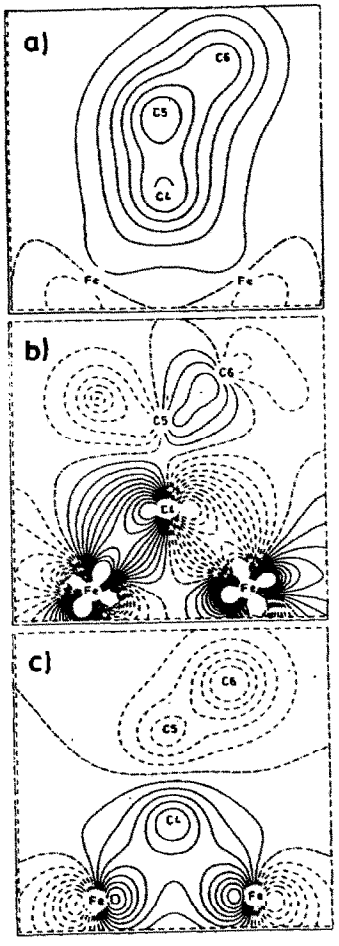

Fig. 6. (a) A contour plot 0.75 Å above the yz plane of the lowest energy occupied π-molecular orbital in the planar conformation. Solid and dashed lines represent positive and negative values. (b) A contour plot in the yz plane of the second lowest energy occupied vinylcarbyne π-molecular orbital. (c) A contour plot 0.50 Å above the y_z plane of the highest energy occupied vinylcarbyne π-molecular orbital in the planar conformation.

iron (Fig. 7c). Thus, rotation of the vinyl group does not destroy conjugation of the vinyl group to the carbyne carbon; the carbyne carbon merely uses a different p orbital to interact with the vinyl group. Similarly, rotation of the vinyl group does not destroy conjugation of the bridging carbyne carbon with the two iron centers. The carbyne carbon p_x orbital (which formed bonding and antibonding combinations with the vinyl group in the planar conformation) forms a π-bond to the iron centers in the perpendicular conformation.

The conjugation between the vinyl group and the carbyne carbon is manifested primarily in the three orbitals for each conformation shown in Figs. 6 and 7, but there are minor contributions to conjugation from many other delocalized molecular orbitals. The net overlap population between the carbyne carbon p_x orbital and the p_x orbital of the α vinyl carbon atom summed over all occupied molecular orbitals provides a quantitative measure of the conjugation between the bridging carbon and the vinyl unit. In the planar conformation, the net overlap population between the

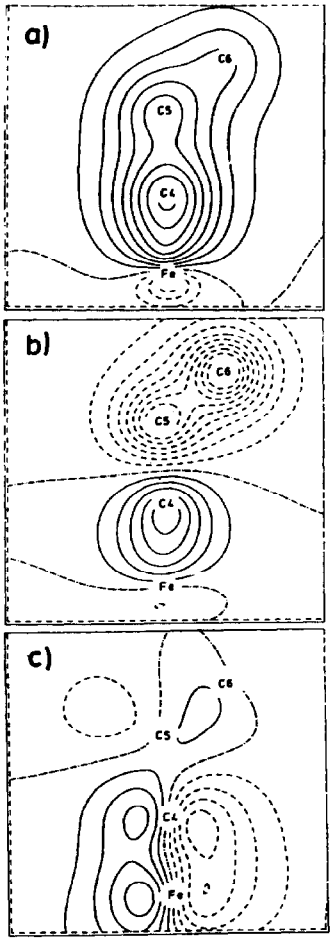

Fig. 7. (a) A contour plot 0.75 Å above the xy plane of the lowest energy occupied vinylcarbyne π-molecular orbital in the perpendicular conformation. Solid and dashed lines represent positive and negative values. (b) A contour plot 0.50 Å above the xy plane of the second lowest energy occupied vinylcarbyne π-molecular orbital in the perpendicular conformation. (c) A contour plot 0.50 Å above the xy plane of the highest energy vinylcarbyne π-molecular orbital in the perpendicular conformation.

p_x orbital of the carbyne carbon and the p_x orbital of the α vinyl carbon is 0.178 and the net overlap population between the p_x orbitals of the two vinyl carbons is 0.430. In the perpendicular conformation, the net overlap population between the p_x orbital of the carbyne carbon and the p_z orbital of the α vinyl carbon is reduced to 0.104 while the overlap between the p_z orbitals of the vinyl unit rises to 0.481. The greater conjugation between the carbyne carbon and the vinyl group in the planar conformation explains why this is the preferred conformation seen by X-ray and by NMR. The fact that conjugation is decreased by only 42% upon rotation to the perpendicular conformation is consistent with the unusually low rotational barriers observed for vinyl carbyne complexes. The larger rotation barriers seen in vinyl carbyne complexes with better electron donor substituents is consistent with the idea that the magnitude of the conjugative stabilization of the planar relative to the perpendicular conformation should be increased by electron donor substituents.

Additional insight into the electron donor ability of the vinylcarbyne ligand is

gained by examination of the Mulliken populations on the vinylcarbyne ligand. The Mulliken population of the two vinyl carbons and three vinyl hydrogens in the planar conformation is 10.823 electrons for a net positive charge of 0.177, indicating that the vinyl unit acts as an electron donating group. When the vinyl unit is rotated by 90° to the perpendicular conformation, the Mulliken population is 10.906 electrons for a net positive charge of 0.094. Therefore, even in the perpendicular conformation, the Mulliken populations indicate that the vinyl unit is acting as an electron donor group although it is less efficient as an electron donor group than in the parallel conformation by 0.083 electrons. These results help to explain the low barrier to rotation since they indicate that the vinyl group can remain in conjugation and act as a π-donor in both the planar and perpendicular conformations. Qualitatively, the fact that the vinyl group is calculated to be a slightly better electron donor in the planar conformation is consistent with the planar geometry observed by X-ray crystallography.

The low barrier to rotation in vinylcarbyne complexes can also be understood in terms of stabilization of a perpendicular carbon–carbon double bond by the diiron unit. Schleyer has suggested that perpendicular conformations of carbon–carbon double bonds, which he calls anti-van't Hoff structures, might be more easily achieved in transition metal systems [11*]. For example, the energy difference between planar and perpendicular conformations of the coordinatively unsaturated vinylidene complex $(CO)_6Fe_2(\mu\text{-}C{=}CH_2)$ was calculated to be small.

Experimental

^1H NMR spectra were obtained on a Bruker WP270 or AM500 spectrometer operating at 270 and 500 MHz respectively. ^{13}C NMR spectra were obtained on an AM500 spectrometer operating at 126 MHz. Acetone-d_6 was dried over B_2O_3. THF-d_8 was dried over Na and benzophenone. Acetonitrile-d_3 was dried over P_2O_5 or 4 Å molecular sieves and stored over CaH_2. Samples for low temperature DNMR were prepared by condensing in acetone-d_6 or THF-d_8 under high vacuum and sealing under a stream of N_2 at room temperature. Samples for high temperature DNMR were prepared by condensing in acetonitrile-d_3 under high vacuum and flame sealing under 500 mm Hg of N_2 at −196 °C. Samples for variable temperature were allowed to equilibrate a minimum of ten minutes between temperature changes before data acquisition. Temperatures were repeatedly calibrated with a platinum resistance wire or from the chemical shift differences in a methanol standard using an experimentally derived curve. Temperatures are estimated to be accurate to within ±1 °C. Line shape analyses were performed using the program DNMR5 [12].

$[C_5H_5(CO)Fe]_2(\mu\text{-}CO)(\mu\text{-}C\text{-}E\text{-}CH{=}CHC_6H_4\text{-}p\text{-}CH_3)^+BF_4^-$ (2). ^1H NMR (500 MHz, acetone-d_6, −100 °C) δ 10.36 (d, J 14.9 Hz, 1 H, μ-C–CH), 8.46 (br, 1H, C_6H_4), 8.16 (d, J 14.9 Hz, 1H, μ-C-CH=C*H*), 8.03 (br, 1H, C_6H_4), 7.54 (br, 2H, C_6H_4), 5.76 (s, 10H, C_5H_5), 2.41 (s, 3H, CH_3). (−28 °C) δ 10.26 (d, J 14.9 Hz, 1H, μ-C–CH), 8.22 (d, J 8.2 Hz, 2H, C_6H_4), 8.12 (d, 14.9 Hz, 1H, μ-C–CH=C*H*), 7.49 (d, J 8.2 Hz, 2H, C_6H_4), 5.67 (s, 10H, C_5H_5), 2.45 (s, 3H, CH_3).

$[C_5H_5(CO)Fe]_2(\mu\text{-}CO)(\mu\text{-}C\text{-}E\text{-}CH{=}CHC_6H_4\text{-}p\text{-}OCH_3)^+BF_4^-$ (3). ^1H NMR (270 MHz, acetone-d_6, −104 °C) δ 9.91 (d, J 14.6 Hz, 1H, μ-C–CH), 8.28 (d, J 8.5 Hz, 1H, C_6H_4), 7.93 (d, J 8.5 Hz, 1H, C_6H_4), 7.91 (d, J 14.6 Hz, 1H, μ-C–CH=C*H*),

7.04 (d, J 8.5 Hz, 2H, C_6H_4), 5.56 (s, 10H, C_5H_5), 3.89 (s, 3H, CH_3). (−30°C) δ 10.20 (d, J 14.6 Hz, 1H, μ-C–CH), 8.31 (d, J 8.9 Hz, 2H, C_6H_4), 8.13 (d, J 14.8 Hz, 1H, μ-C–CH=C*H*), 7.23 (d, J 8.9 Hz, 2H, C_6H_4), 5.64 (s, 10H, C_5H_5), 4.00 (s, 3H, CH_3).

$[C_5H_5(CO)Fe]_2(\mu\text{-}CO)(\mu\text{-}C\text{-}E\text{-}CH{=}CHC_6H_4\text{-}p\text{-}OH)^+BF_4^-$ (4). ^{1}H NMR (270 MHz, THF-d_8, −106°C) δ 10.60 (s, 1H, OH), 10.12 (d, J 14.3 Hz, 1H, μ-C–CH), 8.57 (d, J 7.9 Hz, 1H, C_6H_4), 8.16 (d, J 7.7 Hz, 1H, C_6H_4), 8.08 (d, J 14.3 Hz, 1H, μ-C–CH=C*H*), 7.06 (d, J 7.4 Hz, 1H, C_6H_4), 6.99 (d, J 7.8 Hz, 1H, C_6H_4), 5.58 (s, 10H, C_5H_5). (25°C) δ 9.99 (d, J 14.3 Hz, 1H, μ-C–CH), 9.76 (br, 1H, OH), 8.24 (d, J 7.8 Hz, 2H, C_6H_4), 7.91 (d, J 14.3 Hz, 1H, μ-C–CH=C*H*), 6.96 (d, J 7.8 Hz, 2H, C_6H_4), 5.44 (s, 10H, C_5H_5).

$[C_5H_5(CO)Fe]_2(\mu\text{-}CO)(\mu\text{-}C\text{-}E\text{-}CH{=}CHC_6H_4\text{-}p\text{-}N(CH_3)_2^+BF_4^-$ (5). ^{1}H NMR (270 MHz, acetone-d_6, −95°C) δ 10.00 (d, J 13.7 Hz, 1H, μ-C–CH), 8.45 (dd, J 9.5, 1.9 Hz, 1H, C_6H_4), 8.09 (d, J 13.7 Hz, 1H, μ-C–CH=C*H*), 8.01 (dd, J 9.3, 1.9 Hz, 1H, C_6H_4), 7.16 (dd, J 9.3, 2.3 Hz, 1H, C_6H_4), 7.07 (dd, J 9.2, 2.5 Hz, 1H, C_6H_4), 5.57 (s, 5H, C_5H_5), 5.56 (s, 5H, C_5H_5) 3.36 (s, 3H, CH_3), 3.32 (s, 3H, CH_3). (77°C) δ 9.94 (d, J 13.8 Hz, 1H, μ-C–CH), 8.17 (d, J 9.2 Hz, 2H, C_6H_4), 8.06 (d, J 13.8 Hz, 1H, μ-C–CH=C*H*), 7.05 (d, J 9.3 Hz, 2H, C_6H_4), 5.47 (s, 10H, C_5H_5), 3.35 (s, 6H, CH_3). ^{13}C NMR (126 MHz, acetone-d_6, −76°C) δ 91.44 (s, C_5H_5), 91.05 (s, C_5H_5), (−34°C) 91.17 (s, C_5H_5).

$[C_5H_5(CO)Fe]_2(\mu\text{-}CO)(\mu\text{-}C\text{-}E\text{-}CH{=}CHOCH_2CH_3)^+BF_4^-$ (6). ^{1}H NMR (270 MHz, acetone-d_6, −110°C) Major δ 9.19 (d, J 10.7 Hz, 1H, μ-C–CH); 8.83 (d, J 10.7 Hz, 1H, μ-C–CH=C*H*); 5.60 (s, 5H, C_5H_5); 5.58 (s, 5H, C_5H_5); 4.87, 4.82 (AB part of ABX_3, J_{AB} 10.0 Hz, $J_{AX} = J_{BX} = 7.0$ Hz, 2H, CH_2); 1.43 (t, J 7.0 Hz, 3H, CH_3); minor δ 9.40 (d, J 11.4 Hz, 1H, μ-C–CH), 8.68 (d, J 11.4 Hz, 1H, μ-C–CH=C*H*), 5.64 (s, 5H, C_5H_5), 5.61 (s, 5H, C_5H_5), 4.55 (m, 2H, CH_2), 1.47 (t, J 7.0 Hz, 3H, CH_3). (−28°C) δ 9.23 (d, J 11.0 Hz, 1H, μ-C–CH), 8.70 (d, J 11.0 Hz, 1H, μ-C–CH=C*H*), 5.54 (s, 10H, C_5H_5), 4.79 (q, J 7.1 Hz, 2H, CH_2), 1.52 (t, J 7.1 Hz, 3H, CH_3). Spectra also contain resonances at δ 3.58 and 1.73 due to a half molecule THF of crystallization.

$[C_5H_5(CO)Fe]_2(\mu\text{-}CO)(\mu\text{-}C\text{-}E\text{-}CH{=}CHN(CH_3)_2)^+BF_4^-$ (7). ^{1}H NMR (270 MHz, acetonitrile-d_3, 52°C) δ 8.54 (d, J 11.1 Hz, 1H, μ-C–CH), 7.98 (d of septets, J 11.1, 0.8 Hz, 1H, μ-C–CH=C*H*), 5.16 (s, 5H, C_5H_5), 5.14 (s, 5H, C_5H_5), 3.57 (d, J 0.7 Hz, 3H, CH_3), 3.49 (d, J 0.8 Hz, 3H, CH_3). (112°C) δ 8.56 (d, J 11.1 Hz, 1H, μ-C–CH), 8.02 (d, J 11.1, 1H, μ-C–CH=C*H*), 5.15 (s, 10H, C_5H_5), 3.57 (s, 3H, CH_3), 3.49 (s, 3H, CH_3).

Acknowledgment

Support from the National Science Foundation is gratefully acknowledged. We thank Professor Richard F. Fenske for helpful discussions. MSK thanks SOHIO for a fellowship. SRM thanks W.R. Grace Company for a fellowship.

References

1 C.P. Casey, M.S. Konings, R.E. Palermo, R.E. Colborn, J. Am. Chem. Soc., 107 (1985) 5296.
2 C.P. Casey, S.R. Marder, Organometallics, 4 (1985) 411.
3 C.P. Casey, M.S. Konings, S.R. Marder, J. Organomet. Chem., 345 (1988) 125.

4 M.B. Hall, R.F. Fenske, Inorg. Chem., 11 (1972) 768.
5 M. Nitay, W. Priester, M. Rosenblum, J. Am. Chem. Soc., 100 (1978) 3620.
6 (a) C.P. Casey, M.S. Konings, S.R. Marder, Polyhedron, 7 (1988) 881; (b) High and low temperature limiting spectra for ^{1}H and ^{13}C NMR are given in the experimental section.
7 C.P. Casey, M.W. Meszaros, P.J. Fagan, R.K. Bly, S.R. Marder, E.A. Austin, J. Am. Chem. Soc., 108 (1986) 4043.
8 F.A. Bovey, Nuclear Magnetic Resonance Spectroscopy, Academic Press, New York, 1969; Chapter 7.
9 (a) J.M. Bollinger, J.M. Brinich, G.A. Olah, J. Am. Chem. Soc., 92 (1970) 4025; (b) H. Mayr, W. Förner, P.v.R. Schleyer, J. Am. Chem. Soc., 101 (1979) 6032.
10 (a) F.A. Cotton, in M. Jackman (Ed.), Dynamic Nuclear Magnetic Resonance Spectroscopy, Academic Press, New York, 1975, p. 163–201; (b) F.A.L. Anet, M. Ahmad, J. Am. Chem. Soc., 86 (1964) 119.
11 This was pointed out as a sidelight in a paper that established the importance of π-bonding in both the planar and perpendicular forms of $\overline{BHBHCH_2}$. K. Krogh-Jespersen, D. Cremer, D. Poppinger, J.A. Pople, P.v.R. Schleyer, J. Chandrasekhar, J. Am. Chem. Soc., 101 (1979) 4843.
12 D.S. Stephenson, G. Binsch, Quantum Chemistry Program Exchange, 10 (1978) 365.